Science
AAAS

The Genetic Landscape of the Childhood Cancer Medulloblastoma

D. Williams Parsons, *et al.*

Science **331**, 435 (2011);
DOI: 10.1126/science.1198056

This copy is for your personal, non-commercial use only.

If you wish to distribute this article to others, you can order high-quality copies for your colleagues, clients, or customers by clicking here.

Permission to republish or repurpose articles or portions of articles can be obtained by following the guidelines here.

The following resources related to this article are available online at www.sciencemag.org (this infomation is current as of August 1, 2011):

Updated information and services, including high-resolution figures, can be found in the online version of this article at:
http://www.sciencemag.org/content/331/6016/435.full.html

Supporting Online Material can be found at:
http://www.sciencemag.org/content/suppl/2010/12/15/science.1198056.DC1.html

This article **cites 42 articles**, 17 of which can be accessed free:
http://www.sciencemag.org/content/331/6016/435.full.html#ref-list-1

This article has been **cited by** 4 articles hosted by HighWire Press; see:
http://www.sciencemag.org/content/331/6016/435.full.html#related-urls

This article appears in the following **subject collections:**
Medicine, Diseases
http://www.sciencemag.org/cgi/collection/medicine

Downloaded from www.sciencemag.org on August 1, 2011

Science (print ISSN 0036-8075; online ISSN 1095-9203) is published weekly, except the last week in December, by the American Association for the Advancement of Science, 1200 New York Avenue NW, Washington, DC 20005. Copyright 2011 by the American Association for the Advancement of Science; all rights reserved. The title *Science* is a registered trademark of AAAS.

The Genetic Landscape of the Childhood Cancer Medulloblastoma

D. Williams Parsons,[1,2]* Meng Li,[1]* Xiaosong Zhang,[1]* Siân Jones,[1]* Rebecca J. Leary,[1]* Jimmy Cheng-Ho Lin,[1] Simina M. Boca,[3] Hannah Carter,[4] Josue Samayoa,[4] Chetan Bettegowda,[1,5] Gary L. Gallia,[5] George I. Jallo,[5] Zev A. Binder,[5] Yuri Nikolsky,[6] James Hartigan,[7] Doug R. Smith,[7] Daniela S. Gerhard,[8] Daniel W. Fults,[9] Scott VandenBerg,[10] Mitchel S. Berger,[11] Suely Kazue Nagahashi Marie,[12] Sueli Mieko Oba Shinjo,[12] Carlos Clara,[13] Peter C. Phillips,[14] Jane E. Minturn,[14] Jaclyn A. Biegel,[14] Alexander R. Judkins,[16]† Adam C. Resnick,[15] Phillip B. Storm,[15] Tom Curran,[16] Yiping He,[17] B. Ahmed Rasheed,[17] Henry S. Friedman,[17] Stephen T. Keir,[17] Roger McLendon,[17] Paul A. Northcott,[18] Michael D. Taylor,[18] Peter C. Burger,[19] Gregory J. Riggins,[1,5] Rachel Karchin,[4] Giovanni Parmigiani,[20] Darell D. Bigner,[17] Hai Yan,[17] Nick Papadopoulos,[1] Bert Vogelstein,[1]‡ Kenneth W. Kinzler,[1]‡ Victor E. Velculescu[1]‡

Medulloblastoma (MB) is the most common malignant brain tumor of children. To identify the genetic alterations in this tumor type, we searched for copy number alterations using high-density microarrays and sequenced all known protein-coding genes and microRNA genes using Sanger sequencing in a set of 22 MBs. We found that, on average, each tumor had 11 gene alterations, fewer by a factor of 5 to 10 than in the adult solid tumors that have been sequenced to date. In addition to alterations in the Hedgehog and Wnt pathways, our analysis led to the discovery of genes not previously known to be altered in MBs. Most notably, inactivating mutations of the histone-lysine N-methyltransferase genes MLL2 or MLL3 were identified in 16% of MB patients. These results demonstrate key differences between the genetic landscapes of adult and childhood cancers, highlight dysregulation of developmental pathways as an important mechanism underlying MBs, and identify a role for a specific type of histone methylation in human tumorigenesis.

Medulloblastomas (MBs) originate in the cerebellum, have a propensity to disseminate throughout the central nervous system, and are diagnosed in approximately 1 in 200,000 children less than 15 years old each year (*1*). Although aggressive multimodal therapy has improved the prognosis for children with MB, a substantial proportion of patients are currently incurable (*2*). Moreover, survivors often suffer considerable treatment-related morbidities, including neurocognitive deficits related to radiation therapy. New insights into the pathogenesis of these tumors are therefore sorely needed. Gene-based research has identified two subgroups of MBs, one associated with mutated genes within the Hedgehog pathway and the other associated with altered Wnt pathway genes (*3*, *4*). Amplifications of *MYC* and the transcription factor *OTX2* (*5*–*7*), mutations in *TP53* (*8*), and a number of chromosomal alterations have also been identified in MBs. These discoveries have helped define the pathogenesis of MB and have improved our ability to identify patients who might benefit from therapies targeting these pathways. However, most MB patients do not have alterations in these genes, and the compendium of genetic alterations causing MB is unknown.

The determination of the human genome sequence and improvements in sequencing and bioinformatic technologies have recently permitted genome-wide analyses of human cancers. To date, the sequences of all protein-encoding genes have been reported in more than 80 human cancers (*9*–*20*), representing a variety of adult tumors. In this study, we provide a comprehensive sequence analysis of a solid tumor of childhood. Our data point to a major genetic difference between adult and childhood solid tumors and provide new information to guide further research on this disease.

Sequencing strategy. In the first stage of our analysis, which we have called the "discovery screen," 457,814 primers (table S1) were used to amplify and sequence 225,752 protein-coding exons, adjacent intronic splice donor and acceptor sites, and microRNA (miRNA) genes in 22 pediatric MB samples (17 samples extracted directly from primary tumors, 4 samples passaged in nude mice as xenografts, and 1 cell line) (tables S2 and S3). Seven metastatic MBs were selected for inclusion in the discovery screen to ensure that high-stage tumors were well represented in the study. One matched normal blood sample was sequenced as a control. These analyses corresponded to 50,191 transcripts representing at least 21,039 protein-encoding genes present in the Ensembl, Consensus Coding Sequences (CCDS), and RefSeq databases and 715 miRNA genes from the miRBase database. A total of 404,438 primers were described in our previous publications, and an additional 53,376 primers were newly designed to amplify technically challenging genomic regions, miRNAs, or newly discovered Ensembl genes (table S1). The data were assembled for each amplified region and evaluated using stringent quality-control criteria, resulting in the successful amplification and sequencing of 96% of targeted amplicons and 95% of targeted bases in the 22 tumors. A total of 735 megabases (Mb) of tumor sequence data were generated in this manner.

After automated and manual curation of the sequence traces, regions containing potential sequence alterations (single base mutations and small insertions and deletions) not present in the reference genome or single-nucleotide polymorphism (SNP) databases were reamplified in both the tumor and matched normal tissue DNA and analyzed either through sequencing by synthesis on an Illumina GAII instrument or by conventional Sanger sequencing (*21*). This process allowed us to confirm the presence of the mutation in the tumor sample and determine whether the alteration was somatic (i.e., tumor-specific). Additionally, mutations identified in the four xenograft samples were confirmed to be present in the corresponding primary tumors.

Analysis of sequence and copy number alterations. A total of 225 somatic mutations were identified in this manner (Table 1 and table S4). Of these, 199 (88%) were point mutations and the remainder were small insertions, duplications, or deletions, ranging from 1 to 48 base pairs in length. Of the point mutations, 148 (74%) were predicted to result in nonsynonymous changes, 42 (21%) were predicted to be synonymous, and 9 (5%) were located at canonical splice site residues that were likely to alter normal splicing. Of the 225 somatic mutations, 36 (16%) were predicted to prematurely truncate the encoded protein, either through newly generated nonsense mutations or through insertions, duplications, or deletions leading to a change in reading frame. The mutation spectrum observed for MB was similar to those seen in pancreatic,

[1]Ludwig Center for Cancer Genetics and Therapeutics and Howard Hughes Medical Institute, Johns Hopkins Kimmel Cancer Center, Baltimore, MD 21231, USA. [2]Texas Children's Cancer Center and Departments of Pediatrics and Molecular and Human Genetics, Baylor College of Medicine, Houston TX 77030, USA. [3]Department of Biostatistics, Johns Hopkins Bloomberg School of Public Health, Baltimore, MD 21205, USA. [4]Department of Biomedical Engineering, Institute for Computational Medicine, Johns Hopkins Medical Institutions, Baltimore, MD 21218, USA. [5]Department of Neurosurgery, Johns Hopkins University School of Medicine, Baltimore, MD 21231, USA. [6]GeneGo, Inc., St. Joseph, St. Joseph, MI 49085, USA. [7]Beckman Coulter Genomics, Inc., Danvers, MA 01923, USA. [8]Office of Cancer Genomics, National Cancer Institute, National Institutes of Health, Department of Health and Human Services, Bethesda, MD 20892, USA. [9]Department of Neurosurgery, University of Utah School of Medicine, Salt Lake City, UT 84132, USA. [10]Department of Pathology, Division of Neuropathology, University of California–San Diego, San Diego, CA, USA. [11]Department of Neurological Surgery, University of California–San Francisco, San Francisco, CA 94143, USA. [12]Department of Neurology, School of Medicine of University of Sao Paulo, Sao Paulo, Brazil. [13]Pio XII Foundation, Barretos Cancer Hospital, Sao Paulo, Brazil. [14]Department of Pediatrics, The Children's Hospital of Philadelphia, Philadelphia, PA 19104, USA. [15]Division of Neurosurgery, The Children's Hospital of Philadelphia, Philadelphia, PA 19104, USA. [16]Department of Pathology and Laboratory Medicine, The Children's Hospital of Philadelphia, Philadelphia, PA 19104, USA. [17]The Preston Robert Tisch Brain Tumor Center, Pediatric Brain Tumor Foundation Institute, Department of Pathology, and Department of Surgery, Duke University Medical Center, Durham, NC 27710, USA. [18]Division of Neurosurgery and Program in Developmental and Stem Cell Biology, Hospital for Sick Children, University of Toronto, Toronto, Ontario M5G1L7, Canada. [19]Department of Pathology, Johns Hopkins University School of Medicine, Baltimore, MD 21231, USA. [20]Department of Biostatistics and Computational Biology, Dana-Farber Cancer Institute, and Department of Biostatistics, Harvard School of Public Health, Boston, MA, USA.

*These authors contributed equally to this work.
†Present address: Department of Pathology and Laboratory Medicine, Children's Hospital of Los Angeles, Los Angeles, CA 90027, USA.
‡To whom correspondence should be addressed: velculescu@jhmi.edu (V.E.V.); kinzlke@jhmi.edu (K.W.K.); vogelbe@gmail.com (B.V.)

Downloaded from www.sciencemag.org on August 1, 2011

colorectal, glial, and other malignancies (*22*), with 5′-CG to 5′-TA transitions observed more commonly than other substitutions (Table 1). Such transitions are generally associated with endogenous processes, such as deamination of 5-methylcytosine residues, rather than exposure to exogenous carcinogens (*23*).

The distribution of somatic mutations among the 22 MBs is illustrated in Fig. 1. Two key differences were observed in this cancer as compared to the typical adult solid tumor. First, the average number of nonsilent somatic mutations (nonsynonymous missense, nonsense, indels, or splice site alterations) per MB patient was only 8.3, which is fewer by a factor of 5 to 10 than the average number of alterations detected in the previously studied solid tumor types (Table 1). Second, the proportion of nonsense mutations was more than twice as high as expected given the mutation spectra observed in this tumor type ($P < 1 \times 10^{-4}$, chi-squared test), and the relative fraction of nonsense, insertion, and duplication alterations was higher in MBs than in any of the adult solid tumors analyzed (Table 1) (*21*).

We evaluated copy number alterations using Illumina SNP arrays containing ~1 million probes in a set of 23 MBs, including all discovery screen samples. Using stringent criteria for focal amplifications and homozygous deletions, we identified 78 and 125 of these alterations, respectively, in these tumors (tables S5 and S6) (*21*). High-level amplifications indicate an activated oncogene within the affected region, whereas homozygous deletions may signal inactivation of a tumor suppressor gene. The total number of copy number changes affecting coding genes in each tumor is plotted in Fig. 1. Similar to the point mutation data, we found considerably fewer amplifications (an average of 0.4 per tumor) and homozygous deletions (an average of 0.8 per tumor) affecting coding genes than observed in adult solid tumors (which average 1.6 amplifications and 1.9 homozygous deletions) (*18*, *19*, *24*).

We next evaluated a subset of the mutated genes in an additional 66 primary MBs, including both pediatric and adult tumors (tables S2 and S3). This "prevalence screen" comprised sequence analysis of the coding exons of all genes that were either found to be mutated twice or more in the discovery screen or were mutated once in the discovery screen and had previously been reported to be mutated in other tumor types. Nonsilent somatic mutations were identified in 7 of these 15 genes (table S4). In the prevalence screen, the nonsilent mutation frequency was calculated to be 9.5 mutations per Mb, far higher than the rate found in the discovery screen (0.24 mutations per Mb; $P < 0.001$, Fisher's exact test). The ratio of nonsilent to silent mutations in the prevalence screen was 24 to 1, which is more than 5 times as high as the 4.4 to 1 ratio determined in the discovery screen ($P < 0.01$, Fisher's exact test). In addition, 23 of the 50 prevalence screen mutations (46%) were nonsense alterations or insertions or deletions that were expected to truncate the encoded protein. These data suggest that the genes selected for the prevalence screen were enriched for functionally important genes.

Frequent mutation of *MLL2* and *MLL3* in MB. Somatic mutations in tumor DNA can either provide a selective advantage to the tumor cell (driver mutations) or have no net effect on tumor growth (passenger mutations). A variety of methods are available to help distinguish whether a specific gene or individual mutation is likely to be a driver. At the gene level, the passenger probability score corresponds to a metric reflecting the frequency of mutations, including point mutations, indels, amplifications, and homozygous deletions, normalized for sequence context as well nucleotide composi-

Table 1. Summary of somatic sequence mutations in five tumor types.

	Medulloblastoma*	Pancreas†	Glioblastoma‡	Colorectal§	Breast§
Number of samples analyzed	22	24	21	11	11
Number of mutated genes	218	1007	685	769	1026
Number of nonsilent mutations	183	1163	748	849	1112
Missense‖	130 (71.0)	974 (83.7)	622 (83.2)	722 (85)	909 (81.7)
Nonsense‖	18 (9.8)	60 (5.2)	43 (5.7)	48 (5.7)	64 (5.8)
Insertion‖	5 (2.7)	4 (0.3)	3 (0.4)	4 (0.5)	5 (0.4)
Deletion‖	14 (7.7)	43 (3.7)	46 (6.1)	27 (3.2)	78 (7.0)
Duplication‖	7 (3.8)	31 (2.7)	7 (0.9)	18 (2.1)	3 (0.3)
Splice site or untranslated region‖	9 (4.9)	51 (4.4)	27 (3.6)	30 (3.5)	53 (4.8)
Average number of nonsilent mutations per sample	8	48	36	77	101
Observed/expected number of nonsense alterations¶	2.48	1.18	1.00	1.25	1.37
Total number of substitutions#	199	1486	937	893	1157
Substitutions at C:G base pairs					
C:G to T:A**	109 (54.8)	798 (53.8)	601 (64.1)	534 (59.8)	422 (36.5)
C:G to G:C**	12 (6.0)	142 (9.6)	67 (7.2)	61 (6.8)	325 (28.1)
C:G to A:T**	41 (20.6)	246 (16.6)	114 (12.1)	130 (14.6)	175 (15.1)
Substitutions at T:A base pairs					
T:A to C:G**	19 (9.5)	142 (9.6)	87 (9.3)	69 (7.7)	102 (8.8)
T:A to G:C**	14 (7.0)	79 (5.3)	24 (2.6)	59 (6.6)	57 (4.9)
T:A to A:T**	4 (2.0)	77 (5.2)	44 (4.7)	40 (4.5)	76 (6.6)
Substitutions at specific dinucleotides					
5′-CpG-3′**	85 (42.7)	563 (37.9)	404 (43.1)	427 (47.8)	195 (16.9)
5′-TpC-3′**	14 (7.0)	218 (14.7)	102 (10.9)	99 (11.1)	395 (34.1)

*Based on 22 tumors analyzed in the current study. †Based on 24 tumors analyzed in (*18*). ‡Based on 21 nonhypermutable tumors analyzed in (*19*). §Based on 11 breast and 11 colorectal tumors analyzed in (*16*, *17*). ‖Numbers in parentheses refer to percentage of total nonsilent mutations. ¶Ratio of observed to expected nonsense alterations is dependent on mutation spectra in each tumor type (*21*). #Includes synonymous as well as nonsynonymous point mutations identified in the indicated study. **Numbers in parentheses refer to percentage of total substitutions.

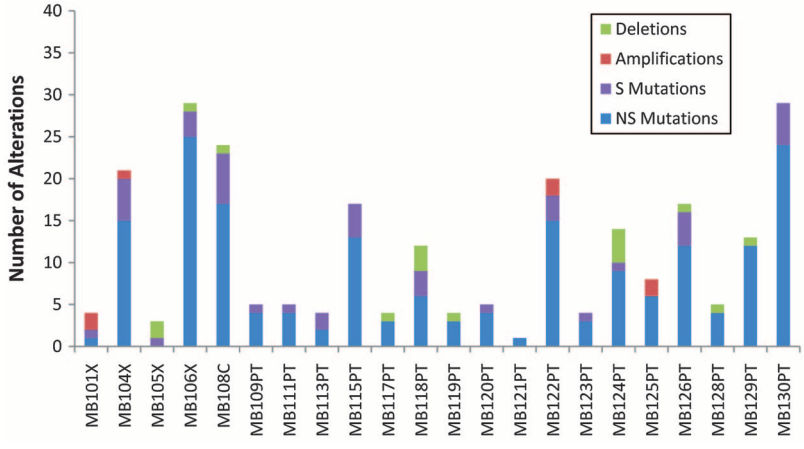

Fig. 1. Number of genetic alterations detected through sequencing and copy number analyses in each of the 22 cancers. NS, nonsilent mutations (including nonsynonymous alterations, insertions, duplications, deletions, and splice site changes); S, silent mutations; deletions, gene-containing regions absent in tumor samples; amplifications, gene-containing regions focally amplified at levels > 10 copies per nucleus (*21*).

Downloaded from www.sciencemag.org on August 1, 2011

tion and length of the gene. The lower the passenger probability score, the less likely it is that mutations in the specific gene represent passengers. Passenger probability scores of the candidate cancer genes (*CAN*-genes) identified in MB are listed in Table 2.

At the individual mutation level, the Cancer-Specific High-Throughput Annotation of Somatic Mutations (CHASM) score is a metric reflecting the likelihood that a missense mutation alters the normal function of the respective protein and provides a selective advantage to the tumor cell (*25*). The CHASM score is based on 73 biochemical features, including conservation of the wild-type amino acid and the mutation's predicted effects on secondary structure. The CHASM score for each mutation observed in this study and the associated *P* value are listed in table S4. Nonsense mutations, as well as small insertions or deletions that disrupt the reading frame, are likely to disrupt function and are assigned a score of 0.001 in this table. About 36% of the evaluated mutations in MB were predicted to disrupt gene function using this approach, a proportion higher than observed in the adult tumor types analyzed to date (*21*).

Finally, we evaluated the discovery screen mutational data (including both sequence and copy number alterations) at a higher "gene set" level. There is now abundant evidence that alterations of driver genes can be productively organized according to the biochemical pathways and biological processes through which they act. The number of gene sets that define these pathways and processes is much less than the number of genes and can provide clarity to lists of genes identified through mutational analyses. In the current study, we used a recently described approach that scores each gene set at the patient rather than the gene level and is more powerful than conventional gene-oriented approaches (*21*, *26*). The most statistically significant pathways and biologic processes highlighted by this gene-set analysis are depicted in table S7. Of these, two—the Hedgehog and Wnt signaling pathways—have been previously shown to play a critical role in MB development. In the Hedgehog pathway, *PTCH1* was mutated in 15 of 88 (17%) tumors, and in the Wnt pathway, *CTNNB1* was mutated in 11 of 88 (13%) tumors (table S4).

Notably, however, the pathways most highly enriched for genetic alterations had not previously been implicated in MB. These involved genes responsible for chromatin remodeling and transcriptional regulation, particularly the histone-lysine N-methyltransferase *MLL2*. Eighteen of the 88 (20%) tumors harbored a mutation in a gene within these pathways or in a related gene member: the histone-lysine-N methyltransferases *MLL2* (mutated in 12 tumors) and *MLL3* (3 tumors); the SWI/SNF–related matrix-associated actin-dependent regulator of chromatin members *SMARCA4* (3 tumors) and *ARID1A* (1 tumor); and the histone lysine demethylase *KDM6B* (1 tumor). The mutations in these genes could be clearly distinguished from passenger alterations. In *MLL2*, for example, 8 of the 12 mutations (67%) were predicted to truncate the encoded proteins as a result of nonsense mutations, out-of-frame indels, or splice site mutations. In contrast, only 32 of the 222 mutations (14%) not affecting core genes of the Hedgehog, Wnt, or *MLL2*-related pathways (*PTCH1*, *CTNNB1*, *MLL2*, *MLL3*, *SMARCA4*, *ARID1A*, and *KDM6B*) resulted in predicted protein truncations ($P < 0.001$, Fisher's exact test). The probability that by chance alone 11 of the 15 mutations in the two histone methyltransferase genes would cause truncations is very small ($P < 0.001$, binomial test). All truncating mutations in *MLL2* and *MLL3* were predicted to result in protein products lacking the key methyltransferase domain (Fig. 2). These data not only provide strong evidence that these pathways are important to MBs, but they also show that *MLL2* and *MLL3* are, on the basis of genetic criteria, tumor suppressor genes that are inactivated by mutation.

Discussion. These data provide a comprehensive view of a solid tumor arising in children. The most impressive difference between this tumor type and those affecting adults is the number of genetic alterations observed. This result could not have been predicted on the basis of previous evidence (*27*). In fact, at the karyotypic level, the incidence of chromosomal changes in MBs is often described as high as that in adult solid tumors [reviewed in (*27*)].

What does the smaller number of mutations reveal about the tumorigenesis of MBs? Most mutations observed in adult tumors are predicted to be passenger alterations (*19*). Passenger mutations provide an evolutionary clock that precisely records the number of divisions that a cell has undergone during both normal development and tumor progression. Therefore, the cell division number is linearly related to the number of passenger mutations detected in a tumor (*28*). This concept is consistent with the positive correlation we identified between increasing patient age and the number of mutations found in their MBs. This relationship was observed for both the mutations detected in the exomes of the discovery screen tumors ($r = 0.73$, $P < 0.01$) and the number of alterations observed in the subset of 15 genes analyzed in the discovery and prevalence screen samples ($r = 0.32$, $P < 0.01$) (tables S8 and S9). Even if we assume that all but one of the mutations in each MB is a passenger, the number of passenger mutations in MBs is still substantially smaller than the number of passenger mutations in adult solid tumors (*16*–*19*), implying that a smaller number of cell divisions is required to reach clinically detectable tumor size in MBs. These data therefore suggest that fewer driver mutations are required for MB tumorigenesis and that driver mutations in MB confer a greater selective advantage than those of adult solid tumors.

Previously, most insights into the molecular basis of MB emerged from the study of hereditary tumor syndromes (*27*), including Gorlin syndrome, caused by germline mutations of *PTCH1*; Turcot syndrome, caused by germline mutations of *APC*; and Li-Fraumeni syndrome, caused by germline mutations of *TP53*. In our study, we found both *PTCH1* and *TP53* to be somatically mutated in MBs (Table 2 and table S4) at frequencies similar

Table 2. Medulloblastoma *CAN*-genes.*

Gene	Number of mutations	Number of amplifications	Number of deletions	Passenger probability
PTCH1	22 / 88	0 / 23	0 / 23	<0.001
MLL2	12 / 88	0 / 23	0 / 23	<0.001
CTNNB1	11 / 88	0 / 23	0 / 23	<0.001
TP53	6 / 88	0 / 23	0 / 23	<0.001
MYC	0 / 88	3 / 23	0 / 23	<0.001
PTEN	3 / 88	0 / 23	0 / 23	0.008
OTX2	0 / 88	2 / 23	0 / 23	0.015
SMARCA4	3 / 88	0 / 23	0 / 23	0.104
MLL3	3 / 88	0 / 23	0 / 23	0.104

**CAN*-genes were defined as those having at least two nonsilent alterations in the samples analyzed. Passenger probabilities were calculated as described in (*21*). The denominators refer to the number of tumors evaluated: 88 tumors were sequenced for mutations, and 23 tumors were analyzed for copy number alterations.

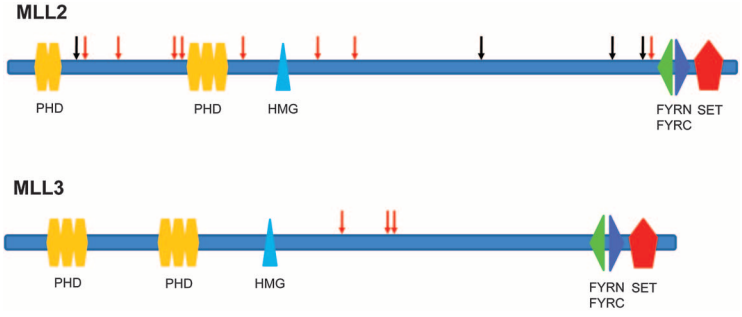

Fig. 2. Somatic mutations in *MLL2* and *MLL3* genes. Nonsense mutations and out-of-frame insertions and deletions are indicated as red arrows; missense mutations are indicated as black arrows. PHD, plant homeodomain finger; HMG, high mobility group box; FYRN, FY-rich N-terminal domain; FYRC, FY-rich C-terminal domain; SET, Su(var)3-9 Enhancer-of-zeste Trithorax methyltransferase domain.

Downloaded from www.sciencemag.org on August 1, 2011

to those observed in earlier studies. We also identified amplifications of *MYC* and *OTX2*, both previously implicated in MB (*5*–*7*).

The ability to investigate the sequence of all coding genes in MBs has also revealed mutated genes not previously implicated in MBs (table S4). Among these, *MLL2* and *MLL3* were of greatest interest, because the frequency of inactivating mutations unequivocally establishes them as MB tumor suppressor genes. This genetic evidence is consistent with functional studies showing that knock-out of murine *MLL3* results in ureteral epithelial cancers (*29*). These genes are large and have been reported in the Catalogue of Somatic Mutations in Cancer (COSMIC) database to be altered in occasional cancers, but not at a sufficiently high frequency to distinguish them from passenger alterations (and with no evidence of a high fraction of inactivating mutations) (*30*). Interestingly, inactivating germline mutations of *MLL2* have recently been identified as a cause of Kabuki syndrome, a multiple malformation disorder without known cancer predisposition (*31*).

The general role of genes controlling histone methylation has become increasingly recognized as a common feature of human cancers. For example, inactivating mutations of the histone H3K27 demethylase gene *UTX* have been observed in multiple myelomas, esophageal cancers, and renal cell cancers (*32*). In addition, a small fraction of renal cell cancers contain mutations in the histone methyltransferase gene *SETD2* and the histone demethylase gene *JARID1C* (*33*), and the histone methyltransferase gene *EZH2* has been found to be mutated in non-Hodgkin's lymphomas (*34*). Most recently, frequent mutations of the chromatin remodeling gene *ARID1A* have been discovered in ovarian clear cell carcinomas (*20*, *35*); of note, one *ARID1A* mutation was discovered in our MB patients (table S4). A link between histone methylation genes (although not *MLL2* or *MLL3*) and MB has also previously been hypothesized based on the observation that copy number alterations affecting chromosomal regions containing histone methyltransferases or demethylases occur in a subset of MBs (*36*).

The mechanism(s) through which MLL genes contribute to tumorigenesis are not known, but some clues can be gleaned from the literature. The MLL family of histone H3K4 trimethylases includes seven genes (*MLL1*, *MLL2*, *MLL3*, *MLL4*, *MLL5*, *SET1A*, and *SET1B*) (*37*). MLL family genes have been shown to regulate HOX gene expression (*38*, *39*), and an attractive possibility is that they normally down-regulate *OTX2*, an MB oncogene (6, 7, *40*). Another possibility is suggested by the observation that β-catenin brings MLL complexes to the enhancers of genes regulating the Wnt pathway, thereby activating their expression (*41*). A third possibility is that MLL family genes are important for transcriptional regulation of normal brain development and differentiation (*42*) and that their disruption may lead to aberrant proliferation of precursor cells.

The identification of *MLL2* and *MLL3* as frequently inactivated MB genes supports the concept that MB is fundamentally characterized by dysregulation of core developmental pathways (*43*). Although alterations of classic cancer genes (e.g., *TP53*, *MYC*, and *PTEN*) were also identified in these childhood tumors, our sequence analysis demonstrated that mutations of genes involved in normal developmental processes, such as MLL family genes and Hedgehog and Wnt pathway genes, were much more frequent. The fact that a relatively small number of somatic mutations is sufficient for MB pathogenesis as compared to adult solid tumors provides further evidence that the temporally restricted subversion of normal cerebellar development is critical in the development of these tumors. This is consistent with the observation that the incidence of MB decreases markedly after childhood, with the tumors becoming quite rare after the age of 40 years (*1*). It will be interesting to determine whether genetic alterations in developmental pathways are a key feature of all childhood malignancies.

The development of an improved classification system for MB that could be used to guide targeted risk-adapted therapy to patients is a primary goal of current MB research. The designation of specific histologic subtypes of MB has proven to be of some prognostic value. For example, large-cell/anaplastic MBs, which are aggressive tumors often associated with *MYC* amplification, carry a relatively poor prognosis (*44*), whereas desmoplastic MBs, which frequently have alterations of *PTCH1* or other Hedgehog pathway genes (*4*), are more easily treatable. However, molecular studies have revealed that these histologic subtypes are biologically heterogeneous (*3*); in addition, most MBs are of the classic subtype and do not have defining molecular alterations. Our results add an additional layer of complexity to these classifications. Although activation of the Wnt and Hedgehog pathways are generally considered to define two MB subtypes (*3*), our data revealed that these groups overlap, because two adult MBs were found to contain mutations of both *PTCH1* and *CTNNB1* (tables S2 and S4). Similarly, *MLL2*/*MLL3* mutations do not appear exclusive to any known subset of MBs: Mutations were identified in both pediatric and adult MBs and were found in all histologic subtypes (although they were most common in large-cell/anaplastic MBs) (Table 3 and tables S9 and S10). In addition, the frequency of *MLL2*/*MLL3* mutations was observed to be similar in *PTCH1*- or *CTNNB1*-mutated MBs (4/24, 17%) as compared to MBs without mutations in *PTCH1* or *CTNNB1* (10/64, 16%). Further studies of these genes in larger number of MBs that have been analyzed for pathologic subtypes will be needed to clarify the molecular classification of this tumor.

We conclude that each MB is driven by a small number of driver mutations, and in our cohort, the

Table 3. Characteristics of medulloblastomas with mutations in *MLL2*-related genes.*

Tumor ID	*MLL2* mutation	*MLL3* mutation	*SMARCA4* mutation	*ARID1A* mutation	*KDM6B* mutation	Patient age (years)	MB subtype	*PTCH1* mutation	*CTNNB1* mutation
MB104X	Nonsense	Nonsense				8	Classic		
MB108C			Missense			Unknown	Unknown		
MB115PT	Missense					5	Classic		
MB118PT				Frameshift		9	Classic		Yes
MB124PT	Frameshift					9	Large cell/anaplastic		
MB126PT	Missense					11	Large cell/anaplastic		
MB127PT	Frameshift					10	Unknown		
MB129PT					Nonsense	Unknown	Unknown		
MB130PT	Frameshift					Unknown	Unknown	Yes	
MB135PT	Frameshift					Unknown	Unknown		
MB205PT		Nonsense				11	Classic		
MB216PT	Missense					33	Large cell/anaplastic		
MB231PT			Missense			18	Classic		Yes
MB245PT	Frameshift					9	Classic		
MB246PT	Missense		Missense			7	Classic		Yes
MB249PT		Nonsense				10	Classic		Yes
MB251PT	Frameshift					26	Large cell/anaplastic	Yes	
MB253PT	Nonsense					32	Nodular/desmoplastic		

*All genes reported in the table were determined to be wild type unless otherwise indicated.

Downloaded from www.sciencemag.org on August 1, 2011

gene set most highly enriched for alterations included *MLL2*. However, there are several limitations to our study. Although in a few cases we have identified two or three bona fide cancer genes that are mutated in individual MBs, other cases show no mutations of any known cancer gene and only one alteration of any gene (Fig. 1 and table S4). Several explanations for the relative absence of genetic alterations in occasional MBs can be offered. First, despite the use of classic Sanger sequencing, a small fraction of the exome cannot be examined, either because of a very high GC content or of homology to highly related genes. Second, it is possible that mutations in the noncoding regions of the genome could occur, and these would not be detected. Third, copy-neutral genetic translocations, not evaluated in our study, could be present in those tumors with very few point mutations, amplifications, or homozygous deletions. Fourth, it is possible that low copy number gains or loss-of-heterozygosity (LOH) of specific regions containing histone-modifying genes could mimic the intragenic mutations that we observed (*36*). Finally, it is possible that heritable epigenetic alterations are responsible for initiating some MBs. The last explanation, involving covalent changes in chromatin proteins and DNA, is intriguing given the new data on *MLL2* in this tumor type. It should thus be informative to characterize the methylation status of histones and DNA in MBs with and without *MLL2/MLL3* gene alterations, as well as to determine the expression changes resulting from these gene mutations. These data highlight the important connection between genetic alterations in the cancer genome and epigenetic pathways and provide potentially new avenues for research and disease management in MB patients.

References and Notes

1. F. Giangaspero *et al.*, in *WHO Classification of the Central Nervous System*, H. O. D. N. Louis, O. D. Wiestler, W. K. Cavenee, Eds. (WHO Press, Lyon, France, 2007).
2. W. R. Polkinghorn, N. J. Tarbell, *Nat. Clin. Pract. Oncol.* **4**, 295 (2007).
3. P. A. Northcott *et al.*, *J. Clin. Oncol.*, published online 7 September 2010; 10.1200/JCO.2009.27.4324
4. M. C. Thompson *et al.*, *J. Clin. Oncol.* **24**, 1924 (2006).
5. S. H. Bigner *et al.*, *Cancer Res.* **50**, 2347 (1990).
6. K. Boon, C. G. Eberhart, G. J. Riggins, *Cancer Res.* **65**, 703 (2005).
7. C. Di *et al.*, *Cancer Res.* **65**, 919 (2005).
8. R. L. Saylors 3rd *et al.*, *Cancer Res.* **51**, 4721 (1991).
9. L. Ding *et al.*, *Nature* **464**, 999 (2010).
10. W. Lee *et al.*, *Nature* **465**, 473 (2010).
11. E. R. Mardis *et al.*, *J. Med.* **361**, 1058 (2009).
12. E. D. Pleasance *et al.*, *Nature* **463**, 191 (2009).
13. E. D. Pleasance *et al.*, *Nature* **463**, 184 (2010).
14. S. P. Shah *et al.*, *Nature* **461**, 809 (2009).
15. T. J. Ley *et al.*, *Nature* **456**, 66 (2008).
16. T. Sjoblom *et al.*, *Science* **314**, 268 (2006).
17. L. D. Wood *et al.*, *Science* **318**, 1108 (2007).
18. S. Jones *et al.*, *Science* **321**, 1801 (2008).
19. D. W. Parsons *et al.*, *Science* **321**, 1807 (2008).
20. S. Jones *et al.*, *Science* **330**, 228 (2010).
21. Materials and methods are available as supporting material on *Science* Online.
22. C. Greenman *et al.*, *Nature* **446**, 153 (2007).
23. T. Soussi, C. Béroud, *Hum. Mutat.* **21**, 192 (2003).
24. R. J. Leary *et al.*, *Proc. Natl. Acad. Sci. U.S.A.* **105**, 16224 (2008).
25. H. Carter *et al.*, *Cancer Res.* **69**, 6660 (2009).
26. S. M. Boca *et al.*, *Genome Biol.* **11**, R112 (2010).
27. P. A. Northcott, J. T. Rutka, M. D. Taylor, *Neurosurg. Focus* **28**, E6 (2010).
28. N. Beerenwinkel *et al.*, *PLOS Comput. Biol.* **3**, e225 (2007).
29. J. Lee *et al.*, *Proc. Natl. Acad. Sci. U.S.A.* **106**, 8513 (2009).
30. S. A. Forbes *et al.*, *Nucleic Acids Res.* **38**, D652 (2010).
31. S. B. Ng *et al.*, *Nat. Genet.* **42**, 790 (2010).
32. G. van Haaften *et al.*, *Nat. Genet.* **41**, 521 (2009).
33. G. L. Dalgliesh *et al.*, *Nature* **463**, 360 (2010).
34. R. D. Morin *et al.*, *Nat. Genet.* **42**, 181 (2010).
35. K. C. Wiegand *et al.*, *N. Engl. J. Med.* **363**, 1532 (2010).
36. P. A. Northcott *et al.*, *Nat. Genet.* **41**, 465 (2009).
37. M. Vermeulen, H. T. M. Timmers, *Epigenomics* **2**, 395 (2010).
38. K. I. Ansari, S. S. Mandal, *FEBS J.* **277**, 1790 (2010).
39. K. Agger *et al.*, *Nature* **449**, 731 (2007).
40. D. C. Adamson *et al.*, *Cancer Res.* **70**, 181 (2010).
41. J. Sierra, T. Yoshida, C. A. Joazeiro, K. A. Jones, *Genes Dev.* **20**, 586 (2006).
42. D. A. Lim *et al.*, *Nature* **458**, 529 (2009).
43. R. J. Gilbertson, D. W. Ellison, *Annu. Rev. Pathol.* **3**, 341 (2008).
44. C. G. Eberhart *et al.*, *Cancer* **94**, 552 (2002).

45. We thank J. Ptak, N. Silliman, L. Dobbyn, and M. Whalen for technical assistance with sequencing analyses, and M. Ehinger, D. Satterfield, E. Lipp, D. Lister, and M. J. Dougherty for help with sample preparation and data collection. This project has been funded in part by the National Cancer Institute, National Institutes of Health, under contract HHSN261200800001E. The content of this publication does not necessarily reflect the views or policies of the Department of Health and Human Services, nor does mention of trade names, commercial products, or organizations imply endorsement by the U.S. government. This work was supported by the Virginia and D. K. Ludwig Fund for Cancer Research, Alex's Lemonade Stand Foundation, the American Brain Tumor Association, the Brain Tumor Research Fund at Johns Hopkins, the Hoglund Foundation, the Ready or Not Foundation, the Children's Brain Tumor Foundation, the Pediatric Brain Tumor Foundation Institute, the David and Barbara B. Hirschhorn Foundation, American Association for Cancer Research Stand Up To Cancer Dream Team Translational Cancer Research Grant, Johns Hopkins Sommer Scholar Program, NIH grants CA121113, CA096832, CA057345, CA118822, CA135877, and GM074906-01A1/B7BSCW, NSF grant DBI 0845275, and DOD NDSEG Fellowship 32 CFR 168a. D.W.P. is a Graham Cancer Research Scholar at Texas Children's Cancer Center. Under licensing agreements between the Johns Hopkins University and Beckman Coulter, B.V., K.W.K., and V.E.V. are entitled to a share of royalties received by the university on sales of products related to research described in this paper. N.P., B.V., K.W.K., and V.E.V are cofounders of Inostics and Personal Genome Diagnostics and are members of their Scientific Advisory Boards. N.P., B.V., K.W.K., and V.E.V. own Inostics and Personal Genome Diagnostics stock, which is subject to certain restrictions under university policy. The terms of these arrangements are managed by Johns Hopkins University in accordance with its conflict-of-interest policies.

Supporting Online Material

www.sciencemag.org/cgi/content/full/science.1198056/DC1
Materials and Methods
Tables S1 to S10
References

21 September 2010; accepted 8 December 2010
Published online 16 December 2010;
10.1126/science.1198056

Downloaded from www.sciencemag.org on August 1, 2011

REPORTS

Rotational Symmetry Breaking in the Hidden-Order Phase of URu_2Si_2

R. Okazaki,[1]* T. Shibauchi,[1]† H. J. Shi,[1] Y. Haga,[2] T. D. Matsuda,[2] E. Yamamoto,[2] Y. Onuki,[2,3] H. Ikeda,[1] Y. Matsuda[1]

A second-order phase transition is characterized by spontaneous symmetry breaking. The nature of the broken symmetry in the so-called "hidden-order" phase transition in the heavy-fermion compound URu_2Si_2, at transition temperature T_h = 17.5 K, has posed a long-standing mystery. We report the emergence of an in-plane anisotropy of the magnetic susceptibility below T_h, which breaks the four-fold rotational symmetry of the tetragonal URu_2Si_2. Two-fold oscillations in the magnetic torque under in-plane field rotation were sensitively detected in small pure crystals. Our findings suggest that the hidden-order phase is an electronic "nematic" phase, a translationally invariant metallic phase with spontaneous breaking of rotational symmetry.

A second-order phase transition generally causes a change in symmetry, such as rotational, gauge, or time-reversal symmetry. An order parameter can then be introduced to describe the low-temperature ordered phase with a reduced symmetry. The heavy-fermion compound URu_2Si_2 undergoes a second-order phase transition at T_h = 17.5 K, which is accompanied by large anomalies in thermodynamic and transport properties (*1*–*3*). Because the nature of the associated order parameter has not been elucidated, the low-temperature phase is referred to as the hidden-order phase. It is characterized by several remarkable features. No structural phase transition is observed at T_h. A tiny magnetic moment appears ($M_0 \approx 0.03\mu_B$, where μ_B is the Bohr magneton) below T_h (*4*), but it is far too

[1]Department of Physics, Kyoto University, Kyoto 606-8502, Japan. [2]Advanced Science Research Center, Japan Atomic Energy Agency, Tokai 319-1195, Japan. [3]Graduate School of Science, Osaka University, Toyonaka, Osaka 560-0043, Japan.

*Present address: Department of Physics, Nagoya University, Nagoya 464-8602, Japan.
†To whom correspondence should be addressed. E-mail: shibauchi@scphys.kyoto-u.ac.jp